NMR Analysis Reveals a Positively Charged Hydrophobic Domain as a Common Motif to Bound Acetylcholine and *d*-Tubocurarine†

Y. Fraenkel,‡ J. M. Gershoni,§ and G. Navon*,‡

School of Chemistry and Department of Cell Research and Immunology, Tel-Aviv University, Ramat-Aviv, Tel-Aviv 69978, Israel

Received June 28, 1993; Revised Manuscript Received September 30, 1993®

ABSTRACT: A complete ^1H assignment of *d*-tubocurarine was carried out using 1D and 2D NMR techniques. Geometries of free acetylcholine (ACh) and *d*-tubocurarine were compared with those of the ligands bound to a recombinant cholinergic binding site (Tα184–200 expressed as a fusion protein in *Escherichia coli*). The conformations of the free ligands were determined by NOESY experiments while those of the bound molecules were obtained by transferred NOESY. The complete relaxation matrix was solved yielding distance constraints which were further refined by a σ back-calculation. ACh bound to recombinant Tα184–200 closely resembled the conformation previously reported for ACh bound to the intact receptor. *d*-Tubocurarine in the bound state undergoes extensive induced conformational rearrangements generating a "cup"-shaped structure. A unique positively charged hydrophobic domain is identified as characteristic of both bound cholinergic ligands.

Much of our physiology is regulated by the interactions of small molecules, ligands, and their corresponding protein counterparts, receptors. This process of biorecognition is of great interest and is often studied while focusing on the receptor itself using a variety of experimental strategies. Whereas much of the emphasis has been on the protein, one can learn a considerable amount by studying the ligands and trying to elucidate their geometries in the bound and free state, assuming that the ligand stucture must complement the binding site of the receptor. The production of information pertaining to the geometry of these ligands can be achieved through a number of processes such as analyzing the ligand in the bound and free state in solution as well as studying the crystalline structures of the ligand through X-ray diffraction. The latter may not necessarily be representive of the physiological picture, whereas the structure of the bound ligand is believed to most closely represent the natural state.

Progress in two-dimensional nuclear magnetic resonance spectroscopy (2D NMR)[1] techniques along with advances in computational methods have made the determination of three-dimensional structures of molecules in solution almost routine (Wüthrich, 1986). In this report we describe the analyses of the cholinergic binding site and its interactions with two ligands: the natural neurotransmitter acetylcholine (ACh) and the antagonist *d*-tubocurarine. The cholinergic binding site has been derived from the nicotinic acetylcholine receptor (AChR) which over the years has been extensively studied (Lentz & Wilson, 1988; Galzi et al., 1991). Through systematic biochemical analyses, using recombinant DNA technology or synthetic peptides, the binding site has been ascribed to the region of residues 180–204 of the α-subunit (Neumann et al., 1986; Barkas et al., 1987; Gershoni, 1987; Radding et al., 1988; Wilson & Lentz, 1988). Recently, using NMR techniques, we have shown that recombinant peptides containing the α183–204 sequence of the AChR from various species contain the binding site of the neurotransmitter itself (Fraenkel et al., 1990, 1991b).

ACh can assume a number of conformations. X-ray diffraction analysis of a few agonists and antagonists containing elements of structural rigidity has led Beers and Reich (1970) to propose that ACh is arranged in a linear structure. Using 2D NMR studies, we have previously shown that while free ACh is linear, it assumes a bent conformation when bound to AChR (Behling et al., 1988). Thus the binding process induces a conformational change in the ligand itself.

Here we present results pertaining to the geometrical structures of ACh and the alkaloid poison, derived from plants, *d*-tubocurarine. We have assigned all of the protons of *d*-tubocurarine by conventional 1D and 2D NMR techniques. Transferred 2D NOE (tNOESY) experiments (Clore et al., 1986) on *d*-tubocurarine and ACh bound to recombinant *Torpedo* α184–200 (Tα184–200), solving the complete relaxation matrices (Keepers & James, 1984; Johnston et al., 1986; Mirau, 1988), and using the distance geometry algorithm DSPACE provided a first approximation of the ligand's geometries. These geometries were subjected to an iteration based on a "σ back-calculation" procedure so as to obtain the geometry which is most consistent with the experimental data. We have found that the geometries of ACh and *d*-tubocurarine when free in solution are very different than those bound to Tα184–200. From these studies, a common structural motif has been found for both ACh and *d*-tubocurarine in their bound state. This motif consists of a positively charged hydrophobic domain.

MATERIALS AND METHODS

Materials. The preparation of the recombinant cholinergic binding site corresponding to Tα184–200 has been previously described (Aronheim et al., 1988). ACh and α-bungarotoxin (BTX) were purchased from Sigma, and *d*-tubocurarine was from Fluka Chemie AG. They were all used without further

† This research was supported by Grant No. 90-00341 from the USA–Israel Binational Science Foundation (BSF), Jerusalem, Israel, to G.N.

‡ School of Chemistry.

§ Department of Cell Research and Immunology.

® Abstract published in *Advance ACS Abstracts*, December 15, 1993.

[1] Abbreviations: ACh, acetylcholine; AChR, acetylcholine receptor; BTX, α-bungarotoxin; COSY, correlated spectroscopy, DG, distance geometry; LRCOSY, long range correlated spectroscopy; NMR, nuclear magnetic resonance; NOESY, nuclear Overhauser effect spectroscopy; tNOESY, transferred nuclear Overhauser effect spectroscopy.

0006-2960/94/0433-644$04.50/0

purification. Protein concentrations were 0.1–0.3 mM. ACh and *d*-tubocurarine concentrations were 7 and 3 mM, respectively. BTX was added (2–3-fold excess) to the ligand/protein solution, and an additional phase-sensitive 2D NOE experiment was carried out. Its relaxation matrix was solved yielding the σ and the ρ values of the bound ligand in the presence of BTX.

Structure determinations of free and bound ligands were done at 25 °C, the same temperature at which the binding studies were performed (Fraenkel et al., 1990, 1991b).

NMR Measurements. 1D and 2D spectra were acquired with a Bruker AM360-WB spectrometer equipped with an Aspect 3000 computer. A full assignment of *d*-tubocurarine protons was carried out by the use of spin decoupling, *J–J* coupling, COSY, long-range COSY (LRCOSY), NOESY, and C–H correlation.

Two-Dimensional NOE Experiments. In order to determine interproton distances in free and protein-bound ligands, phase-sensitive 2D NOE (NOESY) experiments (Macura et al., 1981; Bodenhausen et al., 1984) were done with a number of mixing times (τ_m) in the range of 0.15–0.3 s. An additional experiment with $\tau_m = 0$ was done for the calibration of the relaxation matrix.

Relaxation Matrix. The volumes of the peaks in the 2D NOE experiments at any mixing time (τ_m) are given by

$$\mathbf{A} = \mathbf{A}(\tau_m)/\mathbf{A}(\tau_m = 0) = \exp(-\mathbf{R}\tau_m) \quad (1)$$

A is the normalized matrix volume matrix, and $\mathbf{A}(\tau_m = 0)$ and $\mathbf{A}(\tau_m)$ are the peak volumes matrices at times zero and τ_m, respectively. Equation 1 can be rearranged to give

$$-\ln \mathbf{A}/\tau_m = \mathbf{R} \quad (2)$$

The volume matrix (**A**) can be transformed by means of a similarity transformation to a diagonal matrix **D**:

$$\mathbf{D} = \mathbf{X}^{-1}\mathbf{A}\mathbf{X} \quad (3)$$

where **D** is the diagonal matrix of eigenvalues of **A**, and **X** and $\mathbf{X}^{-1}$ are its eigenvector matrix and inverse, respectively. **R** can be computed applying the "back-transformation" on the resulting diagonal matrix D (eq 3).

$$-\mathbf{X}\ln(\mathbf{D})\mathbf{X}^{-1}/\tau_m = \mathbf{R} \quad (4)$$

Diagonalizations of the volume matrices were preformed using IMSL10. The resulting cross-relaxation rates (σ) obtained from the relaxation matrix were directly used for calculating the internuclear distances (r) among different *resonance groups* observed in the NMR spectrum. This was achieved by scaling with a σ of a proton pair whose internuclear distance is known (Noggle & Schirmer, 1971):

$$(\sigma_{kl}n_{ij})(n_{kl}\sigma_{ij}) = (r_{ij}/r_{kl})^6 \quad (5)$$

n_{ij} and n_{kl} are the different number of protons involved in each resonance group.

Geometry Calculations. Distance geometry (DG) calculations were performed with DSPACE (D. Hare Inc., Version 4.0). A distance bounds matrix was created on the basis of the covalent structure of ACh and *d*-tubocurarine together with the distance constraints derived from the relaxation matrix. Methyls were entered as groups of three hydrogen atoms with their known distances and angles. In the algorithm used, the distance constraints were applied initially for a single pair of the hydrogen atoms i_a and j_b, of the two interacting groups *i* and *j*, yielding an initial geometry. From the resulting geometry, all distances from each proton in the *i* group to each proton in the *j* group were entered to eq 5, obtaining values of σ^{cal}. The result of summation over all the protons in the group yielded a value that was compared with the experimental σ value for the *i–j* interaction. In case of a discrepancy, the calculated geometry was discarded and a new one was calculated and subjected to a new σ back-calculation. Thus the correct geometry must fulfill the following condition for all *i–j* interactions in the molecule:

$$1/(n_{ij})\sum_{a,b=1}^{a,b} i_a j_b \sigma^{cal} = \sigma_{ij}^{exp} \quad (6)$$

Every calculation was done by subjecting the structure to a few cycles of minimizing, annealing, and minimizing again so as to obtain a structure whose penalty function value was minimal. Typically, 20 structures for every geometrical determination were studied. The reported structure represents that in which the average σ value is the closest to the experimental one.

Table 1: Intergroup Distances (Å) in Free and Bound ACh

	free[a]	bound to receptor[a]	bound to Tα184–200
A–B	2.6	2.2	2.3
A–N	3.5	3.2	3.1
A–CH_3	4.1	3.1	3.2
B–N	3.0	3.0	3.0
B–CH_3	4.4	3.1	3.2
CH_3–N	5.5	3.3	3.4
N^+–O[b]	5.1		4.95

[a] Taken from Behling et al. (1988). [b] This is not a constraint, rather this is the outcome of the resulting calculated geometry.

RESULTS

Structure Determination. The relaxation matrix for each system was solved using eqs 2–4. The relaxation matrix obtained consisted of contributions of ligand bound both specifically and nonspecifically to Tα184–200. The contribution of the nonspecific binding was determined by adding excess BTX (2–3-fold), an additional 2D NOE experiment was performed, and the respective relaxation matrix was solved. By subtracting the latter σ values from the former ones, σ values exclusive for specific ligand binding were obtained.

Before studying the *d*-tubocurarine molecule in its free and bound state, it was necessary to convince ourselves that binding to the recombinant peptide Tα184–200 is representative of the binding to the intact receptor. Therefore, the structure of ACh bound to Tα184–200 was compared to our previous results (Behling et al., 1988) in which we analyzed ACh binding to the intact receptor. In the scaling process of the obtained σ values to distance (using eq 5), we followed our previous assumption based on geometrical considerations that the $N(CH_3)_3^+$–NCH_2 distance, 3 Å, is fixed (Behling et al., 1988). Table 1 displays the intergroup distances of free ACh and ACh bound to either AChR or Tα184–200. The most significant observation is the shortening of the distance between the acetyl methyl and the quaternary ammonium group. This is an indication for the bent geometry ACh assumes upon binding. Figure 1 shows the geometry of ACh as a free molecule[2] and when bound to Tα184–200 as calculated by DSPACE together with our "σ back-calculation" iteration. Comparing free vs bound reveals that binding of ACh to

[2] It should be noted that applying our "σ back-calculation" iteration yields a different geometry than that of Behling et al. (1988) although both calculated geometries emerge from the same set of σ values.

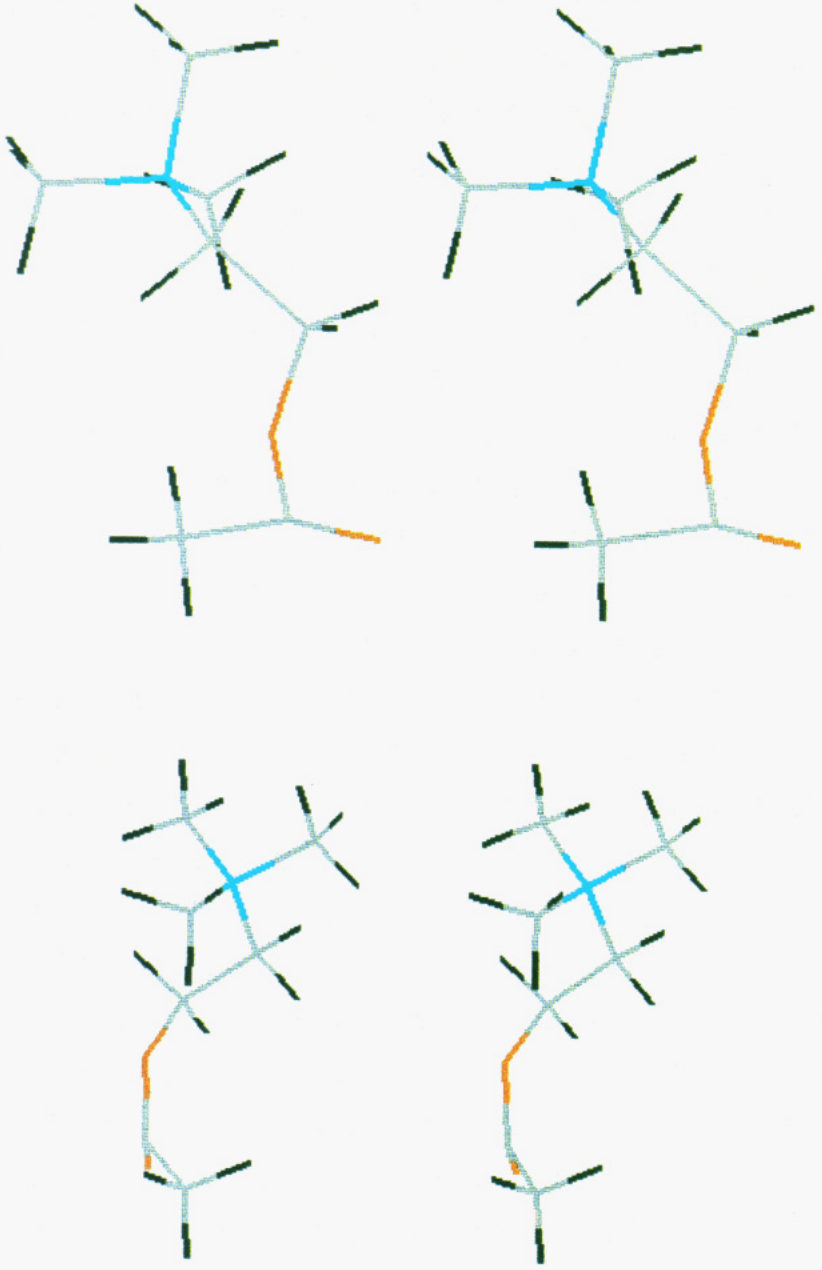

FIGURE 1: Stereoview of ACh geometry as calculated by the distance geometry algorithm DSPACE. (A, bottom) Free ACh in solution [constraints taken from Behling et al. (1988)]. (B, top) ACh bound to the recombinant Tα184–200 sequence (constraints are listed in Table 1). The two geometries are the result of our "σ back-calculation" iteration (see the Materials and Methods).

Tα184–200 indeed induced the characteristic conformational change that was previously observed for ACh binding to the intact receptor. The CH_3 group, as a result of a major change in the dihedral angle of the ester bond [C(=O)–O], is brought closer to the $N(CH_3)_3^+$ group. The obtained geometries illustrate yet another important finding: The N^+–O (carbonyl) distance (listed in Table 1) is about 5 Å both in the free and the bound states[3] (see Discussion).

Proton Assignment in d-Tubocurarine. The two O-methyl groups were assigned on the basis of simple electronic effect arguments. Thus H9a,b,c are at a slightly higher field (3.90 ppm) than H28a,b,c (3.98 ppm). The assignment of the N-methyl groups was done using the LRCOSY experiment. The presence of a cross peak (denoted by an arrow in Figure 3) identifies the two methyl groups at 2.96 and 3.02 ppm as the two methyls of the N1 ammonium group. Thus the remaining methyl group at a lower field (3.15 ppm) is the N2 methyl group.

LRCOSY was further used to distinguish between the two AA′BB′ spin systems in the aliphatic region. Figure 3 displays the complete LRCOSY map revealing a cross peak between the singlet at 7.1 ppm and some resonance at 3.98 ppm and a cross peak between the singlet at 6.96 ppm with some resonance at 3.9 ppm. Note that these two resonances of the two O-methyls overlap with other resonances. These two resonances at 3.98 and 3.9 ppm which interact with the 7.1 and 6.96 ppm resonances were attributed to H4a,b and H22a,b. An interaction between 7.1 and 6.96 ppm with H9a,b,c and H28a,b,c, respectively (that is, a cross peak between the aromatic resonances and the two O-methyls), is not likely to be detected in LRCOSY since they are separated by five bonds. The two resonances of H4a,b and H22a,b have cross peaks in the LRCOSY spectra with their neighboring CH_2 groups, namely, H3a,b and H21a,b, respectively.

[3] A fact that does not seem to us a coincidence, as the same phenomenon occurs with ACh bound to the Tα186–198 sequence and to the human α183–204 sequence (Fraenkel, 1991).

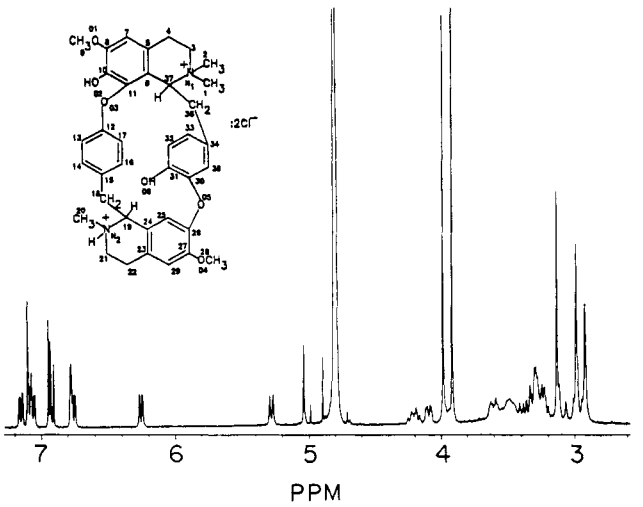

FIGURE 2: Chemical structure of *d*-tubocurarine with our numbering together with the 1D spectrum. For assignment see Table 2. Hydrogen numbering is the same as the carbons to which they are attached. In the case of the methyl groups the three hydrogens are denoted by a, b, and c.

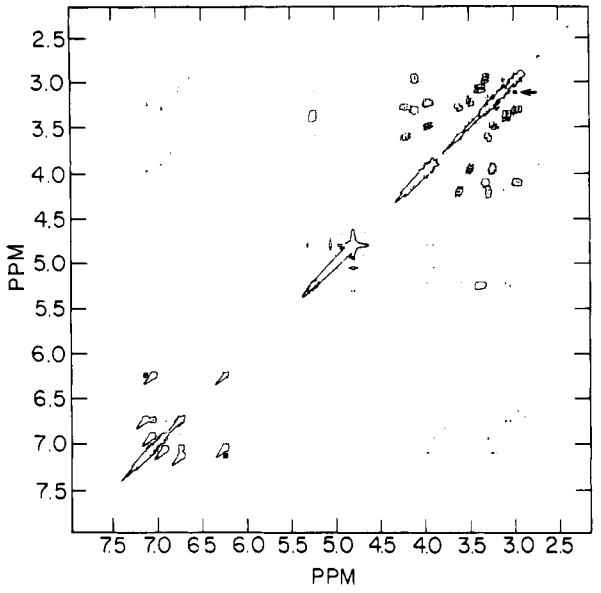

FIGURE 3: Long-range COSY map of *d*-tubocurarine showing important cross peaks between aromatic and aliphatic portions of the spectrum. The cross peak between the two N-methyl groups is denoted with an arrow. Chemical shifts are referenced to the HDO peak at 4.8 ppm. The spectral width was 2100 Hz, and the delay for observing ^4j was 0.08 s corresponding to j = 3.125 Hz.

The 3.98 ppm resonance interacts with the peak at 3.5 ppm, while the 3.9 ppm resonance interacts with the 3.22–3.27 ppm region. Note that up to now we have followed two spin systems with no direct assignment. We have been able to confirm Egan's assignment (Egan et al., 1973) of the 5.24 ppm doublet to H19 by DEPT and CH correlation (data not shown). Therefore the peaks at 3.4 and 3.08 ppm which have cross peaks with the 5.24 ppm doublet must be derived from H18a and H18b. The doublet at 5.24 ppm is unique in its multiplicity being a doublet rather than a double doublet (as is the case for 4.11 ppm, see below). A plausible explanation is that it has a ^3J close to 0 with one of the H18 protons as a result of the dihedral angle between the two. This proton has been identified as H18a on the basis of the geometry obtained through the NOESY experiment (see below). Indeed, looking at the LRCOSY map (Figure 3) reveals that while the resonance at 5.24 ppm has an interaction with the resonance

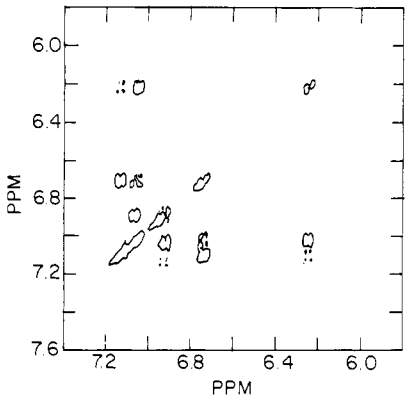

FIGURE 4: Aromatic region of the COSY map of free *d*-tubocurarine demonstrating lack of interaction between the two spin systems ABX and ABCD in the aromatic region.

at 3.4 ppm, it practically has none with the resonance at 3.08 ppm. By default the double doublet at 4.11 ppm can be attributed to H37, and therefore its two cross peaks with the multiplet centered at 3.35 ppm and the region 2.96–3.0 ppm are H36a and H36b. One can observe the residual peak of one of the protons of the CH_2 group between the two methyl groups. This assignment is further substantiated by the existence of a cross peak (LRCOSY) between the N1 methyl groups and the 3.35 ppm resonance.

The existence of a cross peak between the 3.25–3.28 ppm group and the 2.96–3.0 ppm region that consists of the N1 methyls allowed the final assignment. H3a,b are at 3.22–3.27 ppm so that the 3.9 ppm (under the O-methyl) resonances are those of H4a,b. From this it follows that the 6.96 ppm resonance is H7. Consequently, the 7.1 ppm resonance is H29, and thus H22a,b are at 3.98 ppm, and H21a,b are the multiplet at the 3.5 ppm.

Assignment in the aromatic region is somewhat more straightforward. The singlet at 5.08 ppm is attributed to H25, and the explanation for its high-field shift is ring current. We have proved by a CH-correlation experiment that the resonance at 5.08 ppm is an aromatic one. The other two singlets at 6.96 and 7.1 ppm are attributed to H7 and H29, respectively. As for the remaining two phenolic rings, one can observe in an enlarged portion of the aromatic region of a COSY map (Figure 4) that there are two spin systems which are cross-linked internally but do not interact with each other. For example, the double doublet at 6.23–6.25 ppm interacts with the region of 7.11–7.14 ppm but not with the double doublet at 6.73–6.75 ppm. Overlapping ambiguities in this region were resolved through spin decoupling and assignment of J–J values within the groups.

The double doublet at 6.23–6.25 ppm is assigned to H33, which interacts with the resonances at 7.05 ppm attributed to H32 and with that at 7.12 ppm attributed to H35. These three assignments were done on the basis of the J coupling constants 8.5, 2.2, and 0 Hz corresponding to H35–H32, H33–H35, and H32–H35, respectively. The remaining four double doublets are the ABCD protons with the following assignments (based on the fact that $^2J > {}^4J$). H16 is at 6.73–6.75 ppm, H17 is at 7.11–7.14 ppm, H14 is at 7.03–7.07 ppm, and H13 is at 6.92–6.94 ppm. This is based on the observation of a cross peak between 6.73–6.75 ppm with the 3.08 ppm peak of H18a. There are two protons which could be assigned to 6.73–6.75 ppm: H16 and H14. The assignment of this peak to H16 was made possible by the presence of a NOESY cross peak with H25 (see Figure 5). The full assignment of the resonances is given in Table 2.

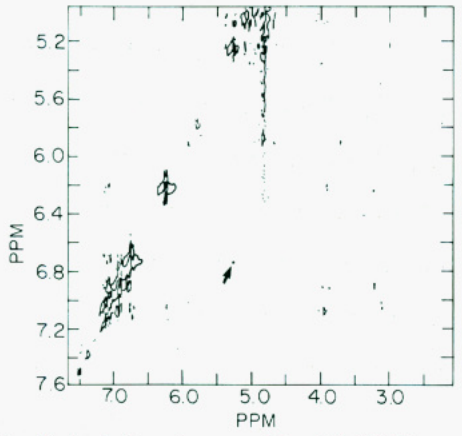

FIGURE 5: Part of the phase-sensitive 2D NOE map of free *d*-tubocurarine revealing lack of cross peak between H16 (6.23–6.25 ppm) and H33 (6.73–6.75 ppm). Chemical shifts are referenced to the HDO peak at 4.8 ppm. The spectral width was 2500 Hz, the mixing time (τ_m) was 0.3 s, and the relaxation delay was 7 s. Gaussian multiplication was done in two dimensions with LB = 2 and GB = 0.03. The arrow denotes a cross peak which does not exist in the bound conformation (compare to Figure 7).

Conformation of Free and Bound d-Tubocurarine. The structure of *d*-tubocurarine molecule when free in solution was determined by carrying out two phase-sensitive NOESY experiments (τ_m = 0 and 0.3 s), solving the relaxation matrix and extracting σ values. Figure 5 is part of the whole NOESY map displaying the aromatic region and a few cross peaks with the aliphatic region. Converting the σ values, extracted from the relaxation matrix, into distances necessitates a scaling factor. In the present system the scaling factor was the σ between the two adjacent aromatic protons H16–H17 (6.73–6.75 with 7.11–7.14 ppm) whose distance was taken as 2.45 Å. As a qualitative check, we have verified that short distances (2.0–2.5 Å) are associated with strong cross peaks and long ones (>3.5 Å) with weak cross peaks (Havel & Wüthrich, 1984). The calculated distances provided distance constraints,

Table 2: Chemical Shift Values (ppm)[a] of the Protons of *d*-Tubocurarine

H1a,b,c	2.96	H22a,b	3.98
H2a,b,c	3.02	H25	5.08
H3a,b	3.22–3.27	H28a,b,c	3.98
H4a,b	3.9	H29	7.1
H7	6.96	H32	7.03–7.05
H9a,b,c	3.9	H33	6.23–6.25
H18a	3.08	H35	7.12
H18b	3.4	H36a	2.98–3.0
H19	5.24	H36b	3.35
H20a,b,c	3.15	H37	4.11
H21a,b	3.5		

[a] Chemical shifts are relative to the HDO peak at 4.8 ppm.

some of which are given in Table 3. These constraints, together with the primary covalent structure, were the input of the distance geometry algorithm DSPACE. All interactions that involve methyl groups were subjected to the "σ back-calculation" iteration. The resulting geometry of free *d*-tubocurarine is displayed in Figure 6. Note that despite differences in detail, the gross structure, i.e., an elongated extended flat molecule, is similar to the two crystalline structures of the dichloride and dibromide previously reported (Codding & James, 1973; Reynolds & Palmer 1976).

The phase-sensitive map (τ_m = 0.2 s) of *d*-tubocurarine when bound to the Tα184–200 sequence exhibits new interactions which indicate a change in *d*-tubocurarine conformation upon binding. The relevant part of the NOESY map is displayed in Figure 7. Four major differences between the maps, in Figures 5 and 7 contributing most significantly to the change in geometry, are specified by arrows. The distance constraints were calculated as above. Those that differ most in comparing bound vs free are given in Table 3. The geometry of bound *d*-tubocurarine was calculated using DSPACE and is shown in Figure 8.

Due to the observation that the N–O distance in bound vs free ACh is not appreciably changed, a similar comparison

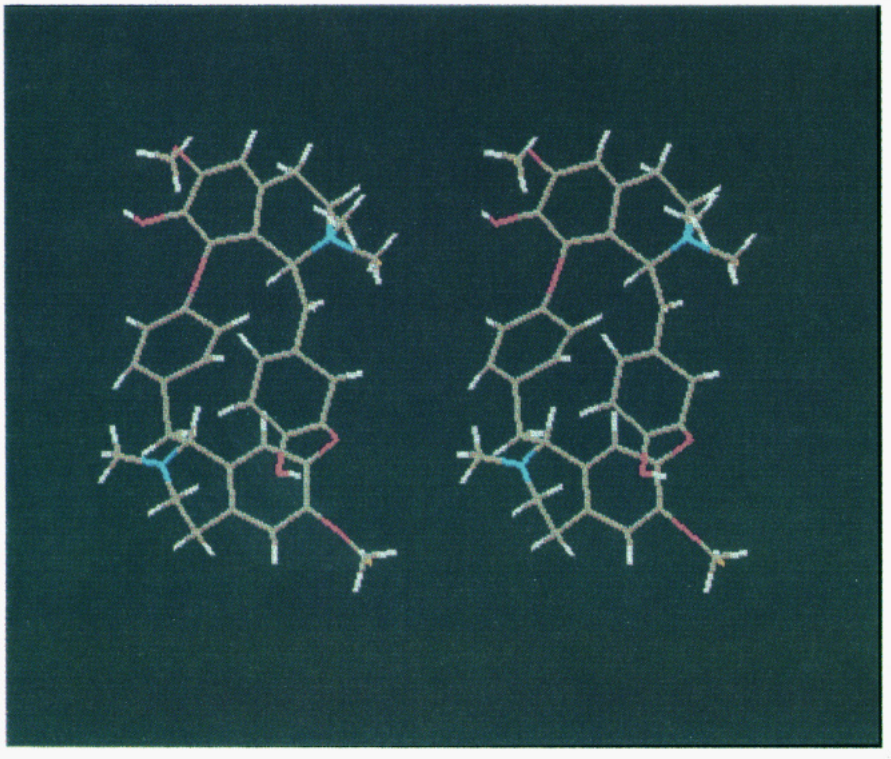

FIGURE 6: Stereoview of *d*-tubocurarine geometry as a free molecule in solution calculated by iterating several geometries by the distance geometry algorithm DSPACE. Distance constraints are listed in Table 3.

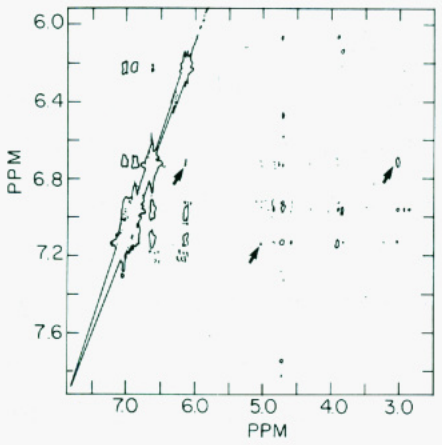

FIGURE 7: Part of the phase-sensitive 2D NOE map of *d*-tubocurarine bound to the Tα184–200 genetically engineered sequence revealing the presence of new cross peaks (denoted by arrows) which do not exist in free *d*-tubocurarine (compare to Figure 5). For the bound *d*-tubocurarine, mixing time (τ_m) was 0.2 s. All other experimental conditions are as listed in the caption of Figure 5 except for the relaxation delay (4 s).

of N–O distances was performed for bound vs free *d*-tubocurarine (Table 4). In this case, note for example that N1–O4 changes from 8.4 to 5.7 Å upon binding of *d*-tubocurarine to Tα184–200.

In summary, these results illustrate that *d*-tubocurarine undergoes marked conformational rearrangements upon its association with Tα184–200. In doing so a hydrophobic positively charged nucleus is formed incorporating both N1 and N2 placing N1 at a 5.7 Å distance from O4. This induced conformational change might create a binding structure which mimics ACh.

DISCUSSION

Rational drug design requires an in-depth understanding of the drug/receptor interaction. Thus the active conformation of the ligand is that of its bound state. Unless the bound geometry is studied, it should be noted that even small differences in the position of key functional groups can have important mechanistic implications. Study of free ligands either in solution or crystals might therefore be misleading. This becomes all the more apparent when dealing with small flexible ligands, in which case their binding site may be

Table 3: Distance Constraints[a] (Å) between Various Hydrogens[b] in Free and Bound *d*-Tubocurarine

interaction	free	bound	interaction	free	bound
H1–H28	>5	3.6	H25–H37	4.4	3.4
H14–H32	3.8	2.7	H14–H25	>5	3.7
H16–H33	>5	2.5	H16–H18a	>5	3.1
H16–H19	3.2	>5	H16–H20	4.8	3.8
H18a–H20	2.1	4.6	H18a–H25	3.8	2.0
H18a–H32	4.5	2.5	H18b–H14	3.9	2.9
H18b–H16	1.9	3.6	H18b–H20	4.5	2.0
H18b–H25	2.5	3.5	H19–H13	3.5	>5
H19–H14	2.5	4.9	H19–H20	4.0	2.7
H19–H22	4.2	3.2	H19–H25	2.3	3.4
H19–H32	1.8	4.6	H19–H33	3.1	>5
H19–H37	4.3	3.4	H36a–H1	4.4	2.1
H36a–H2	4.0	2.0	H36a–H3	2.2	4.5
H36a–H17	3.5	4.7	H36a–H28	>5	2.2
H36b–H1	4.6	3.4	H36b–H2	4.5	2.4
H36b–H17	1.9	3.7	H36b–H28	>5	2.4
H37–H1	2.8	3.6	H37–H3	3.7	2.4
H37–H16	4.5	2.1	H37–H17	3.1	1.9

[a] Using eq 5 together with a scaling factor. [b] For numbering see Figure 2.

Table 4: Nitrogen–Oxygen Distances (Å) in Free and Bound *d*-Tubocurarine

	N1		N2	
	free	bound	free	bound
O1	6.0	6.1	11.5	10.3
O2	5.7	5.9	9.0	8.8
O3	3.8	4.7	7.1	6.5
O4	8.4	5.7	6.3	6.3
O5	6.0	6.3	5.9	6.0
O6	6.9	7.9	5.2	7.0

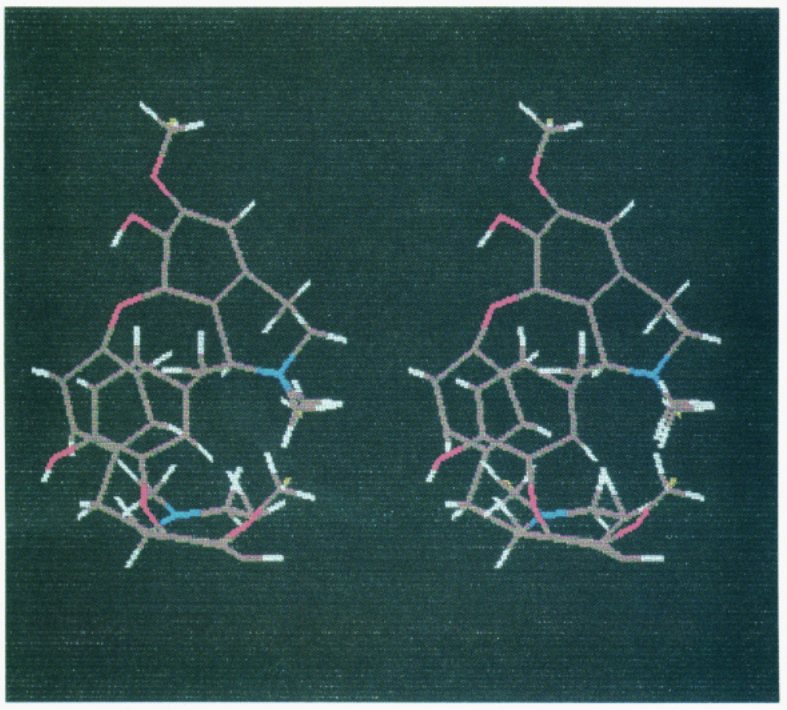

FIGURE 8: Stereoview of *d*-tubocurarine when bound to the Tα184–200 sequence as calculated by DSPACE followed by a several iterations of "σ back-calculation". Distance constraints are listed in Table 3.

regarded as a template that forces the ligand to adopt a certain conformation. In such cases the ligand undergoes induced conformation re-arrangements upon association with its receptor. In solution, structural information concerning the bound ligand is achieved by the tNOE technique (Clore et al., 1986).

The approach adopted in this study was to employ NMR analyses of free *d*-tubocurarine and compare its structure with that bound to a recombinant binding site Tα184–200. This is justified in view of our finding that the ACh geometry bound to intact AChR was found to be very similar to that of ACh bound to Tα184–200 reported here. Indeed both the relaxation matrices and the distance constraints (see Table 1) are practically identical. However, in the present study we extended the geometry calculations beyond the pseudo-atom approach (Tropp & Redfield, 1981) employing the σ back-calculation for the individual protons of the relevant methyls. Applying the technique to bound ACh results in only a slight conformational change compared with that of ACh conformation calculated with the pseudo-atom approach. Nevertheless, this calculation reveals that despite the substantial differences between the free and bound ACh, the N–O(carbonyl) distance remains unaltered in both molecules.[3]

Free *d*-tubocurarine in solution assumes a structure whereby the positively charged ammonium ions repel each other (9.1 Å) maximizing the distance between them. *d*-Tubocurarine association with Tα184–200 induces a dramatic rearrangement of functional moieties. A "cup" is formed bringing both ammonium ions closer together (6 Å) and causing a separation of a hydrophobic cluster from a hydrophilic outer shell (the latter containing all six oxygens). This is brought about by major changes in the dihedral angles of two C–C bonds (C18–C19 and C36–C37) and two ether bonds (C11–O3 and C26–O5). The N1–O4 distance (previously 8.4 Å) is reduced to 5.7 Å, which closely resembles the N–O distance of bound ACh. This structure of the positively charged nitrogen of the quaternary ammonium group at a distance of about 5 Å from an oxygen might in fact mimic the essence of the cholinergic agonists predicted by Beers and Reich (1970). Furthermore, the two methyl groups of the quaternary ammonium group are at a distance of 3.4 and 3.7 Å from the respective O-methyl group, which is very close to that occurring in bound ACh (see Table 1). Thus the characteristic domain found in bound ACh is formed in the *d*-tubocurarine molecule upon binding. Unique to these structures, both that of ACh and *d*-tubocurarine, is the dominance of an ammonium ion buried in a cloud of methyls. Thus characteristic and accentuated in the bound state of cholinergic ligands is the prominence of a positively charged hydrophobic motif. This fits well with our previous findings that both the acetyl methyl and the trimethyl ammonium groups are in a proximity of less than 5 Å from the indole ring of tryptophan-184 of Tα184–200 (Fraenkel et al., 1991a).

Thus, as previously predicted (Dougherty & Stauffer, 1990) and found experimentally by us and others (Dennis et al., 1988; Galzi et al., 1990), a rich π electron aromatic system would complement well a positively charged hydrophobic moiety.

REFERENCES

Aronheim, A., Eshel, Y., Mosckovitz, R., & Gershoni, J. M. (1988) *J. Biol. Chem. 263*, 9933–9937.

Barkas, T., Mauron, A., Roth, B., Alliod, C., Tzartos, S. J., & Ballivet, M. (1987) *Science 235*, 77–80.

Beers, W. H., & Reich, E. (1970) *Nature 228*, 917–922.

Behling, R. W., Yamane, T., Navon, G., & Jelinsky, L. W. (1988) *Proc. Natl. Acad. Sci. U.S.A. 85*, 6721–6725.

Bodenhausen, G., Kogler, H., & Ernst, R. R. (1984) *J. Magn. Reson. 58*, 370–388.

Clore, G. M., Gronenborn, A. M., Carlson, G., & Meyer, E. F. (1986) *J. Mol. Biol. 190*, 259–267.

Codding, P. W., & James, M. N. G. (1973) *Acta Crystallogr. B 29*, 935–942.

Dennis, M., Giraudat, J., Kotzyba-Hibert, F., Goeldner, M., Hirth, C., Chang, J.-Y., Lazure, C., Chretien, M., & Changeux, J.-P. (1988) *Biochemistry 27*, 2346–2357.

Dougherty, D. A., & Stauffer, D. A. (1990) *Science 250*, 1558–1560.

Egan, R. S., Stanaszek, R. S., & Williamson, D. E. (1973) *J. Chem. Soc., Perkin Trans. II*, 716–717.

Fraenkel, Y., (1991) Ph.D. Thesis, Tel-Aviv University. Tel-Aviv, Israel.

Fraenkel, Y., Navon, G., Aronheim, A., & Gershoni, J. M. (1990) *Biochemistry 29*, 2617–2622.

Fraenkel, Y., Gershoni, J. M., & Navon, G. (1991a) *FEBS Lett. 291*, 225–228.

Fraenkel, Y., Ohana, B., Gershoni, J. M., & Navon, G. (1991b) *J. Basic Clin. Physiol. Pharmacol. 2*, 207–215.

Galzi, J.-L., Revah, F., Black, D., Goeldner, M., Hirth, C., & Changeux, J.-P. (1990) *J. Biol. Chem. 265*, 10430–10437.

Galzi, J.-L., Revah, F., Besis, A., & Changeux, J.-P. (1991) *Annu. Rev. Pharmacol. 31*, 37–72.

Gershoni, J. M. (1987) *Proc. Natl. Acad. Sci. U.S.A. 84*, 4318–4321.

Havel, T. F., & Wüthrich, K. (1984) *Bull. Math. Biol. 46*, 673–698.

Johnston, E. R., Dellow, M., & Hendrix, J. (1986) *J. Magn. Reson. 66*, 399–409.

Keepers, J. W., & James, T. L. (1984) *J. Magn. Reson. 57*, 404–426.

Lentz, T. L., & Wilson, P. T. (1988) *Int. Rev. Neurobiol. 29*, 117–160.

Macura, S., Huang, Y., Suter, D., & Ernst, R. R. (1981) *J. Magn. Reson. 43*, 259–281.

Mirau, P. A. (1988) *J. Magn. Reson. 80*, 439–447.

Neumann, D., Barchan, D., Safran, A., Gershoni, J. M., & Fuchs, S. (1986) *Proc. Natl. Acad. Sci. U.S.A. 83*, 3008–3011.

Noggle, J. H., & Schimer, R. E. (1971) *The Nuclear Overhauser Effect*, Academic Press, New York.

Radding, W., Corfield, P. W. R., Levinson, L. S., Hashim, G. A., & Low, B. W. (1988) *FEBS Lett. 231*, 212–216.

Reynolds, C. C., & Palmer, R. A. (1976) *Acta Crystallogr. B32*, 1431–1439.

Tropp, J., & Redfield, A. G. (1981) *Biochemistry 20*, 2133–2140.

Wilson, P. T., & Lentz, T. L. (1988) *Biochemistry 27* 6667–6674.

Wüthrich, K. (1986) *NMR of Proteins and Nucleic Acids*, John Wiley, New York.